Local Buckling of FRP Beams and Columns

By Ever J. Barbero[1] and Ioannis G. Raftoyiannis[2]

Abstract: Fiber-reinforced plastic (FRP) structural members with open or closed thin-walled sections are being used as beams and columns for structural applications where buckling is the main consideration in the design. Analytical models for several local buckling modes under axial and shear loading, taking the flange-web interaction into account, are developed. Experimental data correlating predicted and observed behavior are presented for some commercially available structural shapes. Failure envelopes are developed for box- and I-shape FRP columns and beams. The analytical models presented can be used to predict the behavior of any new pultruted material. The Rayleigh-Ritz method is used in this work to analyze anisotropic flanges of box and I-beams. The anisotropy of the material is introduced by $\pm 45°$ angle-ply layers introduced recently by pultruted manufacturers to improve the buckling strength of columns as suggested by this investigation.

INTRODUCTION

Fiber-reinforced plastic (FRP) beams and columns are being used for civil engineering structural applications. They have many advantages over conventional materials (including steel, concrete, and wood), such as light weight and high corrosion resistance. Mass production of composite structural members (e.g., by pultrusion) makes composite materials cost-competitive with conventional ones.

In the pultrusion process, fibers are pulled through a heated die that provides the shape of the cross section to the final product. Pultrusion is a continuous process of prismatic sections of virtually any shape (*Creative Pultrusions* 1988). Other mass-production techniques, like automatic tape layout, can also be used to produce prismatic sections.

Pultruted structural members have open or closed thin-walled cross sections. For long composite columns, overall (Euler) buckling is more likely to occur before any other instability failure, and the buckling equation has to account for the anisotropic nature of the material. For short columns, local buckling occurs first, leading either to large deflections and finally to overall buckling or to material degradation due to large deflections (crippling). Because of the large elongation to failure allowed by both the fibers (4.8%) and the resin (4.5%), the composite material remains linearly elastic for large deflections and strains, unlike conventional materials that yield (steel) or crack (concrete) for moderate strains. Therefore, buckling is the governing failure for this type of cross section, and the critical buckling load is directly related to the load-carrying capacity of the member (Barbero et al. 1991).

Analytical solutions for the problem of local buckling of the flanges and the webs of pultruted composite beams and columns, taking into account

[1]Asst. Professor, Dept. of Mech. and Aerosp. Engrg., West Virginia Univ., Morgantown, WV 26506-6101.
[2]Grad. Res. Asst., Dept. of Mech. and Aerosp. Engrg., West Virginia Univ., Morgantown, WV.

Note. Discussion open until January 1, 1994. To extend the closing date one month, a written request must be filed with the ASCE Manager of Journals. The manuscript for this paper was submitted for review and possible publication on March 3, 1992. This paper is part of the ***Journal of Materials in Civil Engineering***, Vol. 5, No. 3, August, 1993. ©ASCE, ISSN 0899-1561/93/0003-0339/$1.00 + $.15 per page. Paper No. 3595.

the flange-web interaction, are developed herein. Experimental data correlating predicted and observed behavior are presented.

The problem of local buckling of thin-walled members can be solved by modeling the entire member with finite elements as was done by Vakiener et al. (1991) for orthotropic flanges, by the finite strip method (Cheung 1976), or by coupling the response of flanges and webs individually modeled as plates (Galambos 1988). The coupling of flanges and webs must consider the flexibility of the flange-web connection (Galambos 1988), resulting in a very complex system of equations. In this work, each part of the cross section (flanges and webs) is analyzed independently. The flange-web interaction is modeled as elastic supports on the part being analyzed. The resulting analysis is simple, efficient, and accurate.

An extensive review of analysis techniques for plate buckling is presented by Leissa (1987). Solution techniques for orthotropic flanges, elastically supported on both sides (in the case of the box beam), were presented by Galambos (1988). The solution for an orthotropic plate with one side elastically supported and the opposite side free (case of the I-beam) was presented by Shuleshko (1957). The Rayleigh-Ritz method is used in this work to analyze anisotropic flanges of box and I-beams. The anisotropy of the material is introduced by two thick $\pm 45°$ angle-ply layers introduced recently by pultruted manufacturers to improve the buckling strength of columns as suggested by this investigation [see also Birsa and Taft (1984)].

GOVERNING EQUATIONS

A structural member can be subjected to axial compression, bending, and shear loading. In the case of a beam subjected to bending and shear loading, the flanges are assumed to be under in-plane axial loading and the web under shear loading (Fig. 1). In the case of a column of thin-walled cross section under axial compressive load, it is assumed that the load is uniformly distributed over the cross-section area and that all parts (flanges and webs) are under compression. Under any of these load conditions, the thin walls may buckle locally and can be analyzed as plates with the appropriate boundary conditions. The governing differential equation for buckling of the symmetric anisotropic plate, where no bending-extension coupling exists, under in-plane axial loading and shear loading is

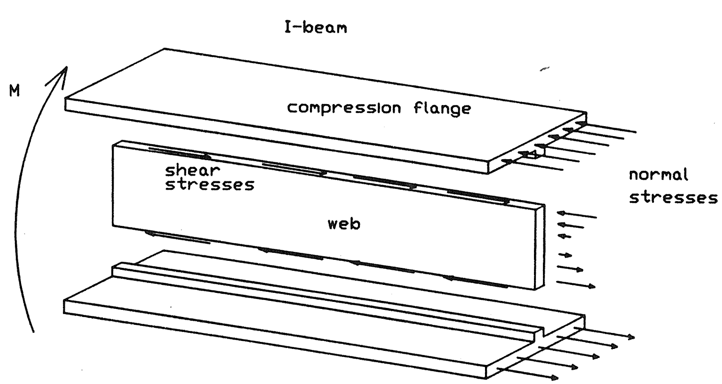

FIG. 1. Representation of I-beam as Separate Flanges and Web

$$D_{11}\frac{\partial^4 w}{\partial x^4} + 4D_{16}\frac{\partial^4 w}{\partial x^3 \partial y} + 2D_{12}\frac{\partial^2 w}{\partial x^2}\cdot\frac{\partial^2 w}{\partial y^2} + 4D_{66}\left(\frac{\partial^2 w}{\partial x \partial y}\right)^2$$

$$+ 4D_{26}\frac{\partial^4 w}{\partial x \partial y^3} + D_{22}\frac{\partial^4 w}{\partial y^4} + N_x\frac{\partial^2 w}{\partial x^2} + 2N_{xy}\frac{\partial^2 w}{\partial x \partial y} = 0 \quad \ldots\ldots\ldots\ldots (1)$$

where D_{ij} = the plate stiffness coefficient; N_x = the in-plane stress resultant; N_{xy} = the shear resultant; and $w(x,y)$ = the buckled shape of the plate. Eq. (1) can be used to solve the local buckling of flange and web under various types of loading by a Levy-type method if no bending-twisting coupling exists ($D_{16} = D_{26} = 0$). In this work, the Rayleigh-Ritz method is used to solve the problem including bending-twisting coupling ($D_{16} \neq 0$, $D_{26} \neq 0$) but is restricted to symmetric laminates. This situation is very common in modern pultruted products (Birsa and Taft 1984). In the Rayleigh-Ritz method, the following energy equation is used instead of (1):

$$\delta V = \int_0^l \int_0^b (D_{11}w_{,xx}\delta w_{,xx} + 2D_{16}w_{,xy}\delta w_{,xx} + 2D_{16}w_{,xx}\delta w_{,xy}$$

$$+ D_{12}w_{,xx}\delta w_{,yy} + D_{12}w_{,yy}\delta w_{,xx} + 4D_{66}w_{,xy}\delta w_{,xy} + 2D_{26}w_{,xy}\delta w_{,yy}$$

$$+ 2D_{26}w_{,yy}\delta w_{,xy} + D_{22}w_{,yy}\delta w_{,yy} + N_x w_{,x}\delta w_{,x} + N_{xy}w_{,x}\delta w_{,y} + N_{xy}w_{,y}\delta w_{,x})$$

$$\cdot dx\, dy + d_1\int_0^l w_{,y}(x,0)\delta w_{,y}(x,0)\, dx + d_2\int_0^l w_{,y}(x,b)\delta w_{,y}(x,b)\, dx = 0$$

$$\ldots\ldots\ldots\ldots\ldots\ldots\ldots\ldots\ldots\ldots\ldots\ldots (2)$$

Setting (2) (first variation of the total potential energy) equal to zero, an eigenvalue problem is obtained for the determination of the critical load N_x. Numerical examples are presented later.

I-BEAMS

The flange of an I-beam can be considered an anisotropic plate connected to the web. The flange-web connection plays significant role in the determination of the critical buckling load. Three cases of flange-web connection shall be considered here: rigid flange-web connection with rigid web (clamped); rigid flange-web connection with flexible web (elastic); and hinged flange-web connection. Previous work (Shuleshko 1957; Holston 1969; Lee 1978; Webber et al. 1985; Raftoyiannis 1991) is based on a Levy-type solution, which is appropriate for materials without bending-twisting coupling terms (D_{16}, D_{26}). For sections that contain $\pm\theta$ layers, it is necessary to use all terms in (2). A Rayleigh-Ritz solution is presented here to determine the critical buckling load for the flange local buckling of I-beams and columns.

The boundary conditions along the flange-web connection are

$$w(x, 0) = 0 \quad \ldots\ldots\ldots\ldots\ldots\ldots\ldots\ldots\ldots (3a)$$

$$M_y(x, 0) = -d_1 w_{,y}(x, 0) \quad \ldots\ldots\ldots\ldots\ldots\ldots\ldots (3b)$$

where d_1 = the stiffness of the web and the flange-web connection combined (Fig. 2). Taking $d_1 = 0$ simulates a hinged flange, which gives a lower bound for the critical load. As d_1 approaches infinity, a clamped flange is simulated, which gives an upper bound for the critical load. A more realistic case for pultruted materials is to have a stiff connection and a flexible web. This case can be simulated by $d_1 = D_{22}^{WEB}$, with the bending stiffness of the web in the transverse direction D_{22}^{WEB} computed by classical lamination theory (Jones 1975). Computation of the coefficient of restraint (Galambos 1988), taking into account the axial load on the restraining plate (the web for the case of an I-section), is not available for anisotropic materials. Furthermore, the analysis presented by Galambos (1988) for isotropic materials assumes rigid connection to the restraining plate (flange-web connection). This may not be the case for pultruted sections that are mainly reinforced along the axis of the beam and have a resin-rich flange-web connection. Measurement of the flange-web connection stiffness, to be added to the coefficient of restraint, is very cumbersome. Based on these considerations, it was decided to conduct the analysis for the limiting cases (hinged and clamped) and for a more realistic case with $d_1 = d_2 = D_{22}^{WEB}$. Finally, buckling-load data obtained experimentally is used to guide the selection of the coefficient of restraint. As shown later using the experimental results for an I-beam, the assumption $d_1 = d_2 = D_{22}^{WEB}$ gives slightly conservative predictions, which indicates that there is some flexibility of flange-web connection and some influence of the compression load on the web.

On the free edge, the following conditions on the bending moment M_y and shear force V_y must be satisfied:

$$M_y(x, b) = V_y(x, b) = 0 \quad (4)$$

They do not need to be imposed on the approximation functions of the Rayleigh-Ritz method. However, for faster convergence, quasi-comparison functions (Meirovich and Kwak 1990) are recommended. The following approximation function is used in this work:

$$w(x, y) = \sum_m \sum_p A_{mp} \sin \frac{m\pi x}{a} \cdot \left(\frac{y}{b}\right)^p \quad (5)$$

Numerical results and correlations with experiments are presented later.

BOX BEAMS

For the case of the box beam, only one half-wave along the width (y-direction, Figs. 2–3) is expected. The boundary conditions that must be satisfied along edges AD and BC (Fig. 3) are

$$w(x, 0) = w(x, b) = 0 \quad (6a)$$

$$M_y(x, 0) = -d_1 w_{,y}(x, 0), \quad M_y(x, b) = d_2 w_{,y}(x, b) \quad (6b)$$

where d_1 and d_2 = constants representing the stiffness of the web and the flange-web connection on side AD and BC (Fig. 3), respectively.

SELECTION OF APPROXIMATION FUNCTION

In the Rayleigh-Ritz method, the solution is approximated by a linear combination of coordinate functions and coefficients. It is well known that the coordinate functions should satisfy the following conditions (Reddy 1984):

1. Satisfy the essential (geometric) boundary conditions but not neces-

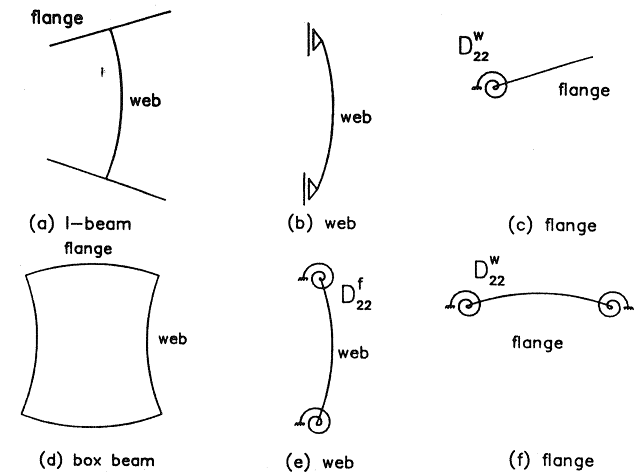

FIG. 2. Equivalent Model of Flange-Web Connection

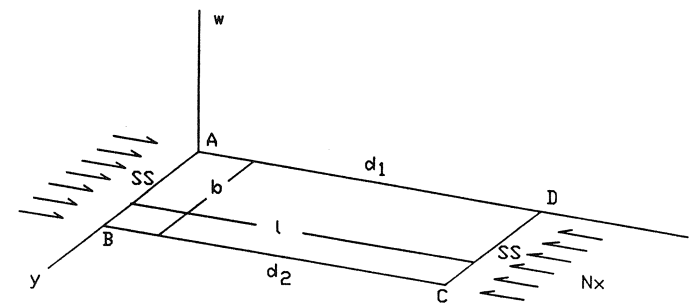

FIG. 3. Equivalent System and Boundary Conditions for Flange of Box Beam

sarily the natural (force) boundary conditions since these are included in the variational statement. However, the linear combination of the coordinate functions should not identically violate the natural boundary conditions. The coordinate functions that satisfy this property were called quasi-comparison functions by Meirovich (1990).

2. Be continuous as required by the variational principle used, which means that the derivatives of the coordinate functions in the variational principle should not identically vanish.

3. Be complete (see Reddy 1984; 1986; Mikhlin and Smolitskiy 1967).

Satisfaction of conditions 1–3 is not enough to guarantee convergence when bending-twisting coupling is present ($D_{16} \neq D_{26} \neq 0$), as shown next.

Consider the flange of a box beam, supported by the two webs with boundary conditions given by (6a) and (6b). An upper bound for the critical load can be found by assuming a clamped boundary (d_1, $d_2 \rightarrow \infty$). The following approximation function satisfies all requirements of the classical Rayleigh-Ritz method.

$$w(x, y) = \sum_m \sum_p a_{mp} \sin \frac{m\pi x}{a} \left(1 - \cos \frac{2p\pi y}{b}\right) \quad \ldots\ldots\ldots\ldots\ldots\ldots\ (7)$$

The coordinate functions in (7) satisfy all the boundary conditions in (6*a*) and (6*b*) (where $d_1, d_2 \rightarrow \infty$ is a complete set), and none of the derivatives in (2) vanish. Even more elaborate (but equivalent) requirements spelled out by Mikhlin and Smolitskiy (1967) are satisfied. Among them, it is worthy to note that the energy integral in (2) obtained using (7) has a finite value. However, all the terms related to D_{16} and D_{26} vanish after integration of (2) if (7) is used. The following function also satisfies conditions 1–3 with $d_1, d_2 \rightarrow \infty$.

$$w(x, y) = \sum_m a_m \sin \frac{m\pi x}{a} \left[\left(\frac{y}{b}\right)^4 - 2\left(\frac{y}{b}\right)^3 + \left(\frac{y}{b}\right)^2\right] \quad \ldots\ldots\ldots\ldots\ (8)$$

where the polynomial is the solution of a clamped-clamped beam. Nonetheless, all terms with D_{16} and D_{26} vanish after integration.

For the case of the elastically supported flange, the following approximation function satisfies conditions 1–3.

$$w(x, y) = \sum_m a_m \sin \frac{m\pi x}{a} \left[\left(\frac{y}{b}\right)^2 - \left(\frac{y}{b}\right)\right] \quad \ldots\ldots\ldots\ldots\ldots\ldots\ (9)$$

but all the terms representing bending-twisting coupling vanish after integration of (2). This would seem to imply that D_{16} and D_{26} have no influence on the buckling load, which is unreasonable, as demonstrated by the use of the following two equations. A doubly sinusoidal approximation of the form

$$w(x, y) = \sum_n \sum_p a_{np} \sin \frac{n\pi x}{a} \sin \frac{p\pi y}{b} \quad \ldots\ldots\ldots\ldots\ldots\ldots\ (10)$$

or a combination like

$$w(x, y) = \sum_n \sum_p a_{np} \sin \frac{n\pi x}{a} \left[\left(\frac{y}{b}\right)^p - \left(\frac{y}{b}\right)\right] \quad \ldots\ldots\ldots\ldots\ldots\ldots\ (11)$$

satisfy all the conditions, and the bending-twisting terms are not canceled after integration. Both (10) and (11) converge to the solution of the elastically restrained boundary, but the convergence of (11) is much faster.

As an specific example, consider an off-the shelf 10-cm by 10-cm by 0.635-cm (4-in. by 4-in. by 1/4-in.) box beam produced by Creative Pultrusions Inc., Alum Bank, Pa. The material properties are given in Appendix I. The material does not have off-axis layers ($D_{16} = D_{26} = 0$). Therefore, the local buckling load can be determined by a Levy-type solution (Shuleshko 1957). To improve the buckling strength of this section, Barbero and Raftoyiannis (1990) proposed replacing all of the randomly oriented, continuous-strand mat layers by angle-ply layers while leaving the unidirectional fiber layers unchanged. The buckling load, as a function of the fiber orientation and the fiber volume fraction of the replacement layers, is shown in Fig. 4. The two solution methods, Levy and Rayleigh-Ritz, are compared. The effect of the bending-twisting coupling is minimal for practical purposes. Further increasing the amount of angle-ply layers would reduce the amount of unidirectional layers, which is unacceptable due to the consequent undesirable reduction of bending stiffness of the member. However, the use of cloth angle-ply layers does allow pultrusion manufacturers to increase the fiber volume fraction of the angle-ply layers without reducing the amount of unidirectional rovings [see also Birsa and Taft (1984)]. In this case, the Rayleigh-Ritz analysis presented elsewhere in this paper becomes necessary.

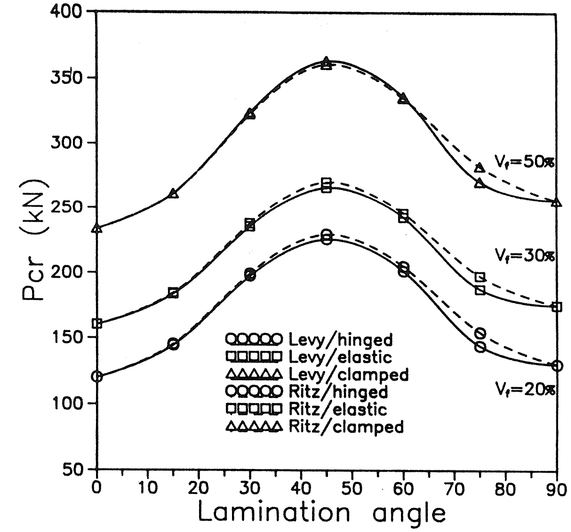

FIG. 4. Comparison between Levy and Rayleigh-Ritz Solutions

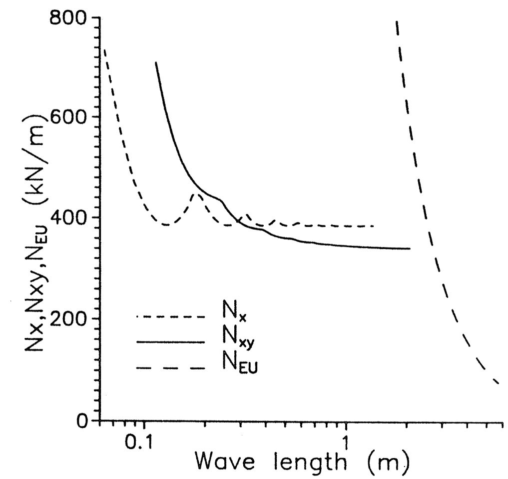

FIG. 5. Failure Envelope for 15-cm by 15-cm by 0.635-cm I-beam including Shear Buckling of Web, Local Buckling of Compression Flange, and Euler Buckling

WEB-SHEAR BUCKLING

Local instability may occur in the web because of shear loading due to bending. When the web is thin or deep, local instability due to shear loading

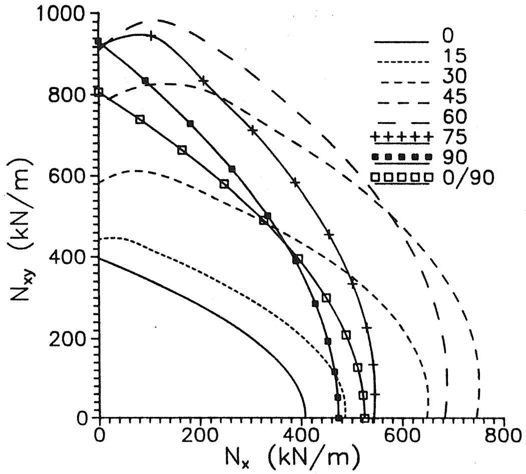

FIG. 6. Interaction Diagram for 15-cm by 15-cm by 0.635-cm I-beam

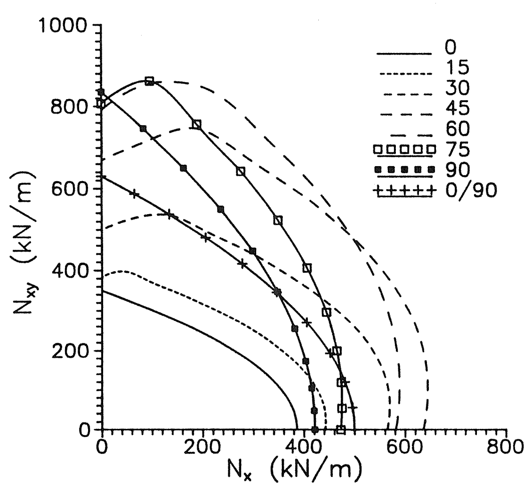

FIG. 7. Interaction Diagram for 10-cm by 10-cm by 0.635-cm Box Beam

may be governing (i.e., occur before flange buckles). The critical shear buckling load for the web can be easily related to the total applied bending load, and the failure envelope for a cross section can be completed (Fig. 5).

In the case of pure bending, the web is subjected to pure shear loading. Presently, the more general case where the edges are elastically supported and a combination of axial and shear loading is applied shall be considered. The governing differential equation for the buckled shape is given by (1). The boundary conditions of the problem are

$$w(0, y) = 0; \quad w(l, y) = 0; \quad w(x, 0) = 0 \quad \text{(12a)}$$

$$w(x, b) = 0; \quad M_x(0, y) = 0; \quad M_x(l, y) = 0 \quad \text{(12b)}$$

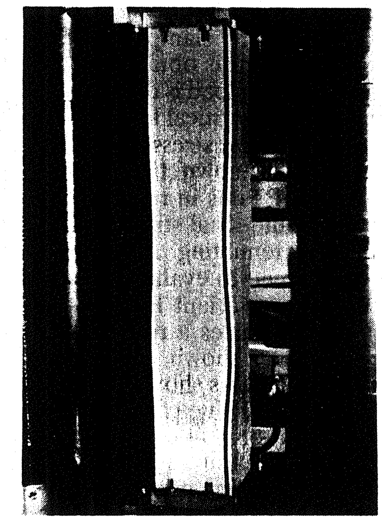

FIG. 8. Experimental Setup Showing Local Buckling of I-beam

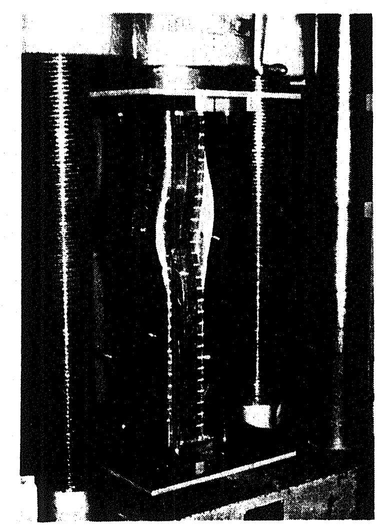

FIG. 9. Experimental Setup Showing Failure of Box Beam

$$M_y(x, 0) = -d_1 w_{,y}|_{y=0}; \quad M_y(x, b) = d_2 w_{,y}|_{y=b} \quad \text{(12c)}$$

The first variation of the total potential energy (Rayleigh-Ritz formulation) is given in (2). The approximate shape function selected for this case is

$$w(x, y) = \sum_m \sum_p a_{mp} \sin\left(\frac{m\pi x}{a}\right) \sin\left(\frac{p\pi y}{b}\right) \quad \text{(13)}$$

This shape function satisfies all boundary conditions except for the case where the boundaries are perfectly clamped (i.e., d_1 and d_2 approach infinity). A linear eigenvalue problem is obtained by introducing (13) into (2). Hence, the critical shear buckling load is determined. By specifying the ratio of axial stress to shear stress, the critical load can be found as a single value. Then, both axial and shear critical stresses can be found.

While the depth of the web is known, the length to consider in the analysis needs further consideration. Beams in real structures may be subjected to a variety of shear, bending, and axial stress distributions, which makes the analysis of all possibilities extenuating. A fixed length was assumed and a parametric study was performed to evaluate the effect of the length on the critical load. The results are invariant for a ratio length (a) to width (b) greater than 5. Axial load produces a repeating buckling pattern with an asymptotic buckling strength as shown in Fig. 5. Shear buckling strength decreases as the length increases, as shown in Fig. 5, but the rate of change is very small and an asymptotic value can be assumed for $a/b > 5$.

The appropriate approximation shape function must be carefully selected. A simply supported boundary condition at ($x = 0, a$) properly accounts for the repeating nature of the buckling pattern.

The connection of the web to the flange is properly modeled as a simple support for an I-beam where the flanges are free to rotate (Fig. 2). For a box, a linearly elastic spring representing the bending stiffness of the flange in the transverse direction is more appropriate (Fig. 2). However, the connection between the web and flange may add additional flexibility (partial, composite action) approaching a hinged boundary.

The buckling shape given by (13) approximates well the buckling mode under shear load. All possible values of buckling of the web under combined shear and compression are given by interaction diagrams, shown in Fig. 6 for an I-beam and in Fig. 7 for a box beam with elastic support. Significant improvement of buckling strength can be obtained by replacing continuous-strand mat layers with angle-ply layers. Furthermore, the optimum angle depends on the shear to compression load ratio. In Fig. 6, a $\pm 60°$ angle produces maximum buckling strength near the pure shear region of the diagram. A $\pm 45°$ angle gives maximum improvement of buckling strength for members primarily loaded in the longitudinal direction (columns) with low shear stresses.

CORRELATION WITH OBSERVED BEHAVIOR

Verification of the predicted critical buckling loads has been carried out through a series of buckling tests described in detail by Raftoyiannis (1991).

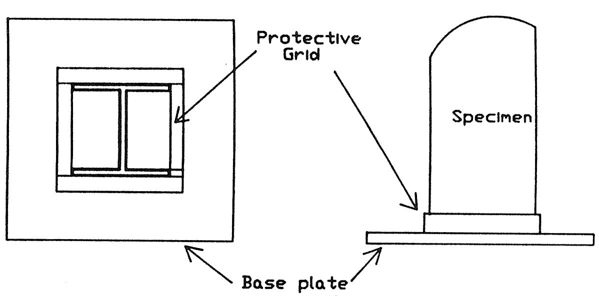

FIG. 10. Experimental Setup Showing Base Plate and Protective Grid

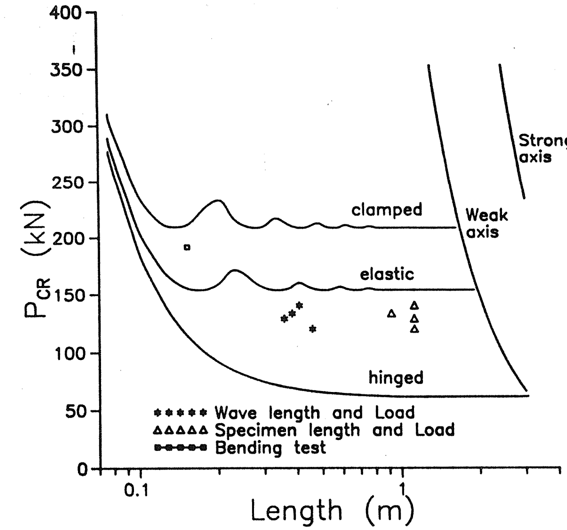

FIG. 11. Correlation between Experimental and Theoretical Results for 15-cm by 15-cm by 0.635-cm Wide-Flange I-beam

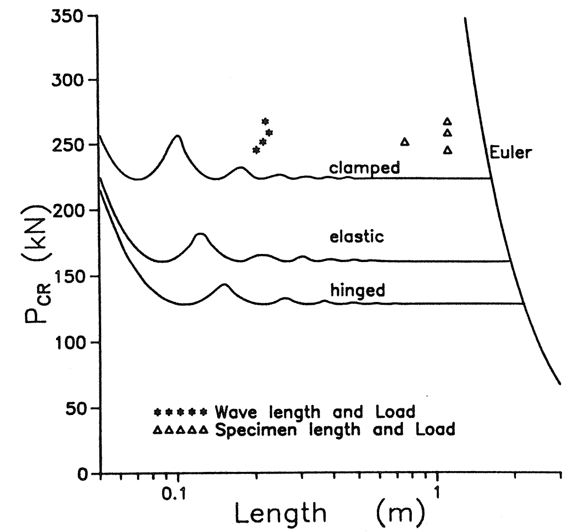

FIG. 12. Correlation between Experimental and Theoretical Results for 10-cm by 10-cm by 0.635-cm Box Beam

Column buckling tests were performed on a universal testing machine of 890-kN (200,000-lb) capacity. Specimens were obtained from pultruted structural shapes produced by Creative Pultrusions. The stacking sequence and fiber volume fractions and properties obtained with the methodology introduced by Barbero (1991) for pultruted materials, are given in Appendix I. Two sections were tested as columns: a 15-cm by 15-cm by 0.635-cm)–

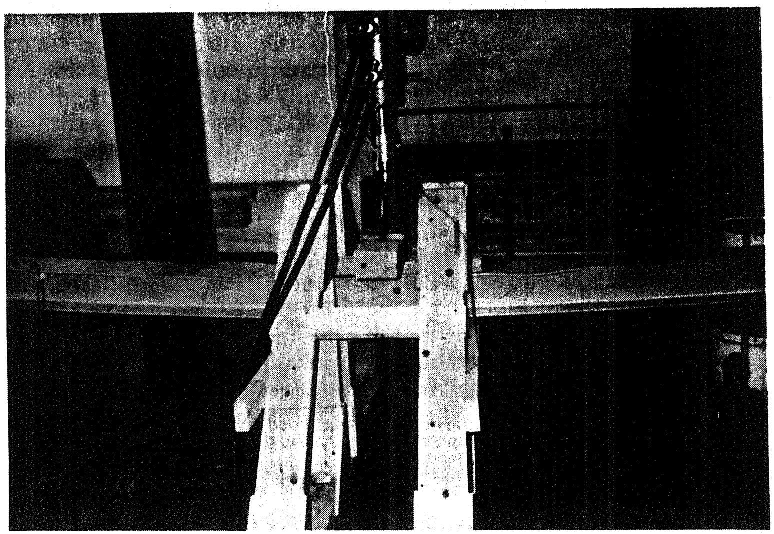

FIG. 13. Bending Test Showing Local Buckling of Compression Flange

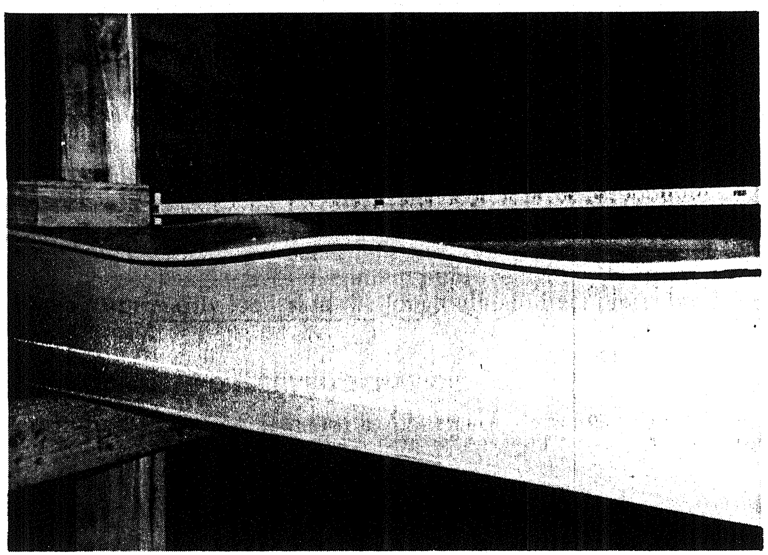

FIG. 14. Close-up of Fig. 13, Showing Measurement of Postbuckling Wavelength

(6-in. by 6-in. by 1/4-in.–) wide flange I-beam (Fig. 8); and a 10-cm by 10-cm by 0.635-cm (4-in. by 4-in. by 1/4-in.–) box beam (Fig. 9). The ends of the columns were clamped to flat plates using 2.5-cm (1-in.) square bars as a safety measure and to ensure proper alignment (Fig. 10). Significant deflections and loss of stiffness were observed (Fig. 8) for wide-flange I-beams.

Box beams show minor deflections and negligible loss of stiffness until failure (Fig. 9), but the failure is clearly of the local buckling type. The

surface of the specimens was marked at 2.5-cm (1-in.) intervals to facilitate measuring the wavelength after buckling. The wavelength can be easily measured during the test. The analytical results (Figs. 11–12) show that the local buckling load is independent of the length for moderate mode number. That is, the local buckling occurs at a constant load with a wave number that accommodates to the actual length of the column. This is confirmed by the experimental data presented here for box and I-columns as well as by the experiments conducted by Yuan et al. (1991) on refrigeration tower columns. The sample size is four, in Figs. 11–12, including the bending tests that give identical results.

Experimental data for the I-beams are shown in Fig. 11 along with theoretical curves. The local buckling curves correspond to three different assumptions about the stiffness of the web and the flange-web connection. A hinged flange [$d = 0$ in (3)] assumes that the flange-web connection is very flexible. Elastic ($d = D_{22}^{WEB}$) assumes that the flange-web connection is rigid but the web is flexible. Clamped ($d \rightarrow \infty$) assumes that both the connection and the web are rigid. Small deflections were observed at low levels of loads. Then, for a wide range of load, no deflections were observed. Finally, significant deflections were observed (Fig. 8) for small increments in the load. At this point the load was recorded, and it is reported in Fig. 11. The data correlate well with the theoretical predictions for elastically supported flange. Buckling occurs with a wavelength shown with triangular symbols in Fig. 11.

Experimental data for the box beams are shown in Fig. 12 along with theoretical curves. The local buckling curves correspond to three different assumptions about the stiffness of the web and the flange-web connection. Hinged flange [$d = 0$ in (6)] assumes that the flange-web connection is very flexible. The experimental data clearly indicate that this is not the case for the specimens tested. Elastic ($d = D_{22}^{WEB}$) assumes that the flange-web connection is rigid but the web is flexible. Clamped ($d \rightarrow \infty$) assumes that both the connection and the web are rigid. The experimental data correspond to the failure load since, for the case of the box beam, it is very difficult to detect the bifurcation load. Therefore, all experimental values are higher than the predicted values. Buckling occurs with a wavelength shown with triangular symbols in Fig. 12.

A 15-cm by 15-cm by 0.635-cm (6-in. by 6-in. by 1/4-in.) wide-flange I-beam was tested in bending (Fig. 13) and buckling of the compression flange was observed. The three-point–bending test was performed using steel rollers to simulate the simply supported boundary conditions. The load was applied with an hydraulic jack and measured with a load cell and a strain indicator. The center deflection was measured with a dial gage. Lateral-torsional buckling was presented by a wooden frame as shown in Fig. 13. The transverse load at which local buckling of the compression flange occurred is used to compute the compressive stress on the top flange at buckling. The equivalent axial load that would produce the same value of buckling stress is reported in Fig. 11. The wavelength measured during the experiment (Fig. 14) corresponds to mode 1, as can be seen in Fig. 12.

CONCLUSIONS

The analytical solutions developed here have been used to predict critical buckling loads as well as the buckling mode. In the case of thin-walled beams and columns, local buckling must be considered. Instability failure of a part of the cross section is important because it initiates a process that leads to the collapse of the member. Prediction of local buckling is therefore important for the prediction of ultimate axial and bending strength of pultruted beam columns.

Novel solutions for elastically supported webs and flanges with bending-twisting coupling have been developed. The effect of the bending stiffness D_{22} of the web on the buckling of the flange was simulated as an elastic support. It is demonstrated analytically that the local buckling load is independent of the length for moderate mode number. That is, the local buckling occurs at a constant load with a wave number that accommodates to the actual length of the column.

The analytical models presented should be used to check for the effect of coupling coefficients in arbitrarily laminated shapes. Significant improvements can be accomplished by including angle-ply layers in pultruted structural shapes. Both web and flange crippling behavior must be accounted for in the optimization process.

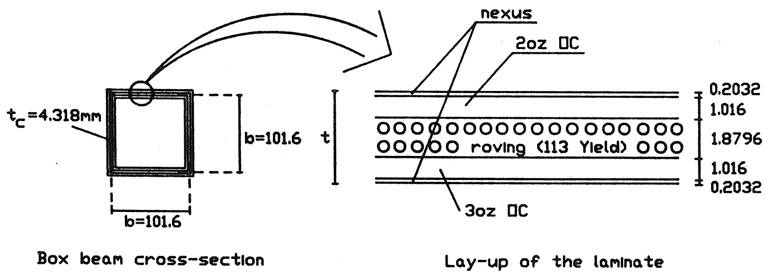

FIG. 15. Lay-up for 10-cm by 10-cm by 0.635-cm Box Beam

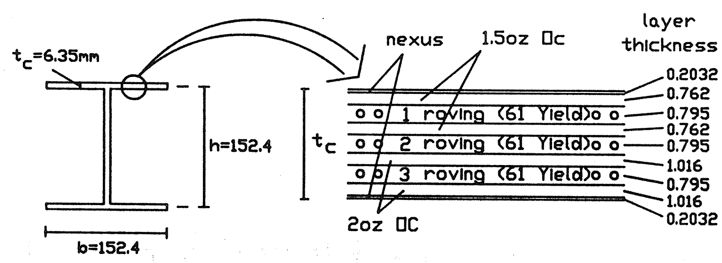

FIG. 16. Lay-up of Flange of 15-cm by 15-cm by 0.635-cm I-beam

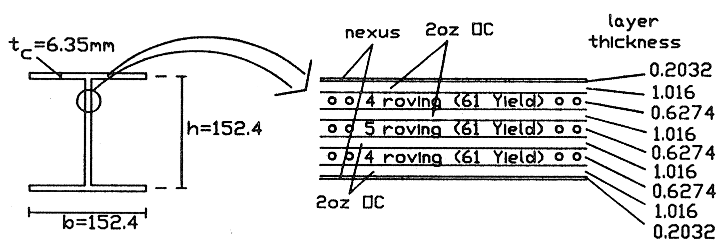

FIG. 17. Lay-up of Web of 15-cm by 15-cm by 0.635-cm I-beam

TABLE 1. Micromechanical Data for 10-cm by 10-cm Box Beam[a]

Layer (1)	E_x (MPa) (2)	E_y (MPa) (3)	ν_{xy} (4)	G_{xy} (MPa) (5)	V_f (%) (6)
Nexus	6,187	6,187	0.40	2,214	10
57-g (2-oz) continuous-strand mat	9,925	9,925	0.42	3,490	23
85-g (3-oz) continuous-strand mat	13,194	13,194	0.43	4,607	34
Roving	32,754	5,725	0.26	2,331	43

[a]The information shown corresponds to material produced in 1989, and is not representative of current structural shapes.

TABLE 2. Micromechanical Data for 15-cm by 15-cm I-beam[a]

Layer (1)	E_x (MPa) (2)	E_y (MPa) (3)	ν_{xy} (4)	G_{xy} (MPa) (5)	V_f (%) (6)
Nexus	6,187	6,187	0.40	2,214	10
42.5-g (1.5-oz) continuous-strand mat	9,925	9,925	0.42	3,490	23
57-g (2-oz) continuous-strand mat	9,925	9,925	0.42	3,490	23
Roving 1	15,808	4,076	0.25	1,662	18
Roving 2	39,278	6,704	0.27	2,724	52
Roving 3	24,781	4,793	0.26	1,952	31
Roving 4	37,209	6,338	0.27	2,579	49
Roving 5	35,140	6,021	0.27	2,448	46

[a]The information shown corresponds to material produced in 1989, and is not representative of current structural shapes.

ACKNOWLEDGMENTS

The financial support of the National Science Foundation (NSF grant 8802265) and the West Virginia Department of Transportation Division of Highways (WVDOH grant RPT699) is appreciated. Special recognition is given to Creative Pultrusions Inc., which provided the samples for the experimental program.

APPENDIX I. MATERIAL PROPERTIES

The material properties of pultruted materials can be predicted from the processing information used by the manufacturer (*Creative Pultrusions* 1988), according to the procedure developed by Barbero (1991) and Raftoyiannis (1991). The internal composition of a box beam is shown in Fig. 15, and the resulting properties are given in Table 1. The stacking sequence of an I-beam is shown in Figs. 16–17, and the resulting properties are given in Table 2.

APPENDIX II. REFERENCES

Barbero, E. J. (1991). "Pultruted structural shapes—From the constituents to the structural behavior." *Sampe J.*, 27(1), 25–30.
Barbero, E. J., and Raftoyiannis, I. (1990). "Buckling analysis of pultruded com-

posite columns." *Impact and buckling of structures*, AD Vol. 20, Am. Soc. of Mech. Engrs., New York, N.Y.
Barbero, E. Y., Fu, S. H., and Raftoyiannis, I. (1991). "Ultimate bonding strength of composite materials." *J. Mater. in Civ. Engrg.*, ASCE, 3(4), 292–306.
Birsa, R., and Taft, P. (1984). "Transverse strength for pultruted parts." *Mater. Engrg.*, 5, 63–64.
Cheung, Y. K. (1976). *Finite strip method in structural analysis*. Pergamon, Oxford, England.
Creative Pultrusions design manual. (1988). Creative Pultrusions Inc., Alum Bank, Pa.
Galambos, T. V. (1988). *Guide to stability design criteria for metal structures*. 4th Ed., John Wiley & Sons, Inc., New York, N.Y.
Holston, A. Jr. (1969). "Buckling of orthotropic plates with one free edge." *AIAA J.*, 8(7), 1352–1354.
Jones, R. M. (1975). *Mechanics of Composite Materials*. Hemisphere, New York, N.Y.
Lee, D. J. (1978). "The local buckling coefficient for orthotropic structural sections." *Aerosp. J.*, 82(575), 313–320.
Leissa, A. W. (1987). "A review of laminated composite plate buckling." *Appl. Mech. Rev.*, 40(5), 575–590.
Meirovich, L., and Kwak, M. K. (1990). "Convergence of the classical Rayleigh-Ritz method and the finite element method." *AIAA J.*, 28(8), 1509–1516.
Mikhlin, S. G., and Smolitskiy, K. L. (1967). *Approximate methods for solution of differential and integral equations*. Elsevier, New York, N.Y.
Raftoyiannis, I. G. (1991). "Buckling of pultruted composite columns," MSCE thesis, West Virginia University, Morgantown, W.V.
Reddy, J. N. (1984). *Energy and variational methods in applied mechanics*. John Wiley & Sons, Inc., New York, N.Y.
Reddy, J. N. (1986). *Applied functional analysis and variational methods in engineering*. McGraw-Hill, New York, N.Y.
Shuleshko, P. (1957). "Reduction method for buckling problems of orthotropic plates." *Aeronaut. Q.*, 8, 145–156.
Vakiener, A. R., Zureick, A., and Will, K. M. (1991). "Prediction of local flange buckling in pultruted shapes by finite element analysis." *Advanced composite materials in civil engineering structures, (Proc. ASCE Specialty Conf.)*, S. L. Iyer, ed., ASCE, 303–309.
Webber, J. P. H., Holt, P. J., and Lee, D. A. (1985). "Instability of carbon fibre reinforced flanges of I section beams and columns." *Composite Struct.*, 4, 245–265.
Yuan, R. L., Hashen, Z., Green, A., and Bisarnsin, T. (1991). "Fiber-reinforced plastic composite columns." *Advanced composite materials in civil engineering structures (Proc. ASCE Specialty Conf.)*, S. L. Iyer, ed., ASCE, 205–211.

APPENDIX III. NOTATION

The following symbols are used in this paper:

a = length of specimen;
b = width of flange or web;
D_{11}, D_{12}, D_{22}, D_{16}, D_{26}, and D_{66} = plate stiffness coefficients;
d_1, d_2 = elastic constants representing web-flange interaction;
E_1, E_2 = modulus of elasticity in local (material) coordinates;
G_{12} = shear modulus in local (material) coordinates;
M_x, M_y, M_{xy} = bending moments;

N_x, N_{xy} = in-plane stress resultants (forces);
V_f = fiber volume fraction;
V_x, V_y = shear forces;
w = transverse deflection; and
ν_{12} = Poisson ration in local (material) coordinates.